Minimax Anti-Jammer Design for FHSS/QPSK Satellite Communication Systems

Mengqi Ren and Ruixin Niu
Department of Electrical and Computer Engineering
Virginia Commonwealth University
Richmond, Virginia 23284, U.S.A.
Email: {renm, rniu}@vcu.edu

Gang Wang and Genshe Chen
Intelligent Fusion Technology, Inc.
Germantown, Maryland 20876, U.S.A.
Email: {gang.wang, gchen}@intfusiontech.com

***Abstract*—In this paper, a minimax anti-jamming strategy in a frequency hopping spread spectrum (FHSS)/quadrature phase-shift keying (QPSK) satellite communication system is developed. The goal of the anti-jammer is to minimize symbol error probability while that of the jammer is to maximize it. The jammer attacks legitimate communication system via two jamming strategies: single-tone jamming and full-band multitone jamming. The jammer maximizes symbol error probability by changing strategies and jamming signal phases. The anti-jammer minimizes symbol error probability by changing decision thresholds when demodulating QPSK signals. The optimal anti-jammer under the worst jamming case is obtained by solving a minimax optimization problem numerically. Numerical results show that when the anti-jammer has no prior knowledge of the phase of the jamming signal, the best decision thresholds are the same as those in the case without attacks. The anti-jammer is able to reduce symbol error probability by increasing signal power or employing more frequency hopping channels. If the jammer knows the anti-jammer's minimax decision thresholds, it is better for the jammer to use single-tone jamming when the jamming power is low or the number of frequency hopping channels is large; when jamming power is high or the number of frequency hopping channels is small, full-band multitone jamming should be used.**

I. Introduction

Jamming attacks are significant threats to satellite communication systems. A jammer can simply interfere the legitimate communication systems by injecting jamming signals into communication channels [1], [2]. As a result, the communication between the transmitter and receiver will be corrupted. To achieve reliable communication, employing anti-jammer is crucial in satellite communication systems. One efficient way to design anti-jammer is adopting frequency hopping spread spectrum (FHSS) [3], [4], which avoids attacks by switching channels from time to time.

In the literature, the performance of phase-shift keying (PSK) with FHSS was studied under various types of jammer attacks. In [5], signals were generated using binary PSK (BPSK) with FHSS. Four types of jamming were investigated and the bit error probability was provided under each type of jamming. In [6], the error probability of quadrature PSK (QPSK) or quadrature amplitude-shift keying (QASK) with FHSS was evaluated, either in the presence of partial-band multitone jamming or partial-band noise jamming. In [7], the performance of a slow frequency-hopped differential PSK system was studied in the presence of jamming and additive white Gaussian noise (AWGN). The performance of any M-ary PSK with FHSS under partial-band multitone jamming was studied in [8]. By assuming that the phase of jamming signal is a random variable, the probability density function (PDF) of the phase difference between received jammed signal and transmitted signal was derived, based on which the bit error probability and the performance expression under worst jamming scenarios were obtained in [8]. In all the above publications, no anti-jammer was considered and the decision thresholds used by the demodulator are fixed. An optimal anti-jammer was designed by solving a maximin optimization problem in [9]. In this maximin optimization problem, the expected detection time at the jammer was minimized respect to the window length used by the jammer's detector and maximized respect to the receiver side signal power.

In this paper, we design an anti-jammer which is optimal under the worst jamming scenario. The FHSS/QPSK is employed to modulate signals. Since the main purpose of satellite communication systems is to transfer signals correctly, the performance of FHSS/QPSK is evaluated by using the symbol error probability. The purpose of the anti-jammer is to minimize the symbol error probability while that of the jammer is to maximize it. To reduce the jammer's effect, the anti-jammer uses FHSS to transmit and receive QPSK signals. The carrier frequency of QPSK signals is hopping between N frequencies according to a predetermined pseudo-random frequency hopping sequence. We assume that the jammer uses the same symbol duration as the transmitter and receiver, and the total jamming power is fixed. For simplicity, we assume that the jammer attacks the legitimate communication system with only two jamming strategies: single-tone jamming—randomly jamming one tone with full power, and full-band multitone jamming—jamming all the N tones and allocating jamming power equally among the N tones. The jamming tones coincide with carrier frequencies of the transmitter and receiver. In the worst jamming case, jammer will use the strategy and jamming phase which cause highest symbol error probability. Therefore, the anti-jammer is designed to minimize symbol error probability under the worst jamming case by changing decision thresholds when the receiver demodulates QPSK signals. So, the anti-jammer

978-1-5090-3781-0/16/$31.00 ©2016 IEEE

needs to solve a minimax optimization problem.

II. Problem Formulation

In this paper, QPSK is used to modulate and demodulate the signals in satellite communication systems. Let $U_k(t)$ be the QPSK signal sent by transmitter, where k is signal index. Assume the jammer attacks the communication systems by jamming interference $J_k(t)$ into the channel. Denote the received signal by $R_k(t)$, which is represented as

$$R_k(t) = U_k(t) + J_k(t) + n(t),\ k = 1, 2, \ldots \tag{1}$$

where $n(t)$ denotes the sample function of the additive white Gaussian noise (AWGN) random process with the power spectral density $S_n(f) = \frac{N_0}{2}$ W/Hz.

The QPSK modulated signal $U_k(t)$ is a frequency hopping signal, which is represented as

$$U_k(t) = p_k(t)\cos(2\pi f_c(k)t + \phi_m(k)) \tag{2}$$

where $f_c(k)$ is the carrier frequency for the kth signal which is changing among N tones $\{f_{c1}, f_{c2}, \ldots, f_{cN}\}$ according to a predetermined pseudo-random frequency hopping sequence. The phase for the kth signal is

$$\phi_m(k) = \frac{(2m-1)\pi}{4},\ m = 1, 2, 3, 4 \tag{3}$$

and $p_k(t)$ is

$$p_k(t) = \sqrt{\frac{2E_s}{T_m}} g_{T_m}[t - (k-1)T_m] \tag{4}$$

where E_s is the energy in each signal, T_m is the signal duration, and $g_{T_m}(t)$ is a rectangular baseband pulse as follows

$$g_{T_m}(t) = \begin{cases} 1, & 0 \leqslant t < T_m \\ 0 & \text{otherwise} \end{cases} \tag{5}$$

Two jamming strategies are considered: single-tone jamming and full-band multitone jamming. The single-tone jamming is randomly jamming one tone with full power at each time. The full-band multitone jamming is jamming all the N tones with equal power. Assuming that the jammer uses the same signal duration T_m, the jamming signal is in one of the following forms

$$\begin{aligned} &\text{Strategy I}: \quad J_k^{\mathrm{I}}(t) = q_k(t)\cos(2\pi f_j(k)t + \theta) \\ &\text{Strategy II}: \quad J_k^{\mathrm{II}}(t) = \textstyle\sum_{i=1}^{N} \frac{q_k(t)}{\sqrt{N}} \cos(2\pi f_{ci}t + \theta) \end{aligned} \tag{6}$$

where $f_j(k)$ is carrier frequency of the kth jamming signal which is randomly picked from the N tones $\{f_{c1}, f_{c2}, \ldots, f_{cN}\}$, the phase θ is deterministic which is chosen from $[0, 2\pi)$, and $q_k(t)$ is

$$q_k(t) = \sqrt{\frac{2E_j}{T_m}} g_{T_m}[t - (k-1)T_m] \tag{7}$$

where E_j is the energy in each jamming signal.

The orthonormal basis functions used by the receiver are

$$\begin{cases} \psi_{1k}(t) = \sqrt{\frac{1}{E_s}} p_k(t)\cos(2\pi f_c(k)t) \\ \psi_{2k}(t) = -\sqrt{\frac{1}{E_s}} p_k(t)\sin(2\pi f_c(k)t) \end{cases} \tag{8}$$

The outputs of QPSK demodulator $\mathbf{y}_m(k)$ contains two signal components $y_{1m}(k)$ and $y_{2m}(k)$, which may be expressed as

$$\mathbf{y}_m(k) = \begin{bmatrix} y_{1m}(k) \\ y_{2m}(k) \end{bmatrix} = \mathbf{s}_m(k) + \mathbf{j}(k) + \mathbf{n}(k) \tag{9}$$

Let $\mathbf{s}_m(k) = \begin{bmatrix} s_{1m}(k) \\ s_{2m}(k) \end{bmatrix}$, $\mathbf{j}(k) = \begin{bmatrix} j_1(k) \\ j_2(k) \end{bmatrix}$, and $\mathbf{n}(k) = \begin{bmatrix} n_1(k) \\ n_2(k) \end{bmatrix}$. The two components of $\mathbf{s}_m(k)$ are

$$\begin{cases} s_{1m}(k) = \sqrt{E_s}\cos(\phi_m(k)) \\ s_{2m}(k) = \sqrt{E_s}\sin(\phi_m(k)) \end{cases} \tag{10}$$

From (10), we know that when the channel is noise-free and jamming-free, the four symbols $\mathbf{s}_m(k)$ $(m = 1, 2, 3, 4)$ form a square in phase quadrature, which is shown in Fig. 1.

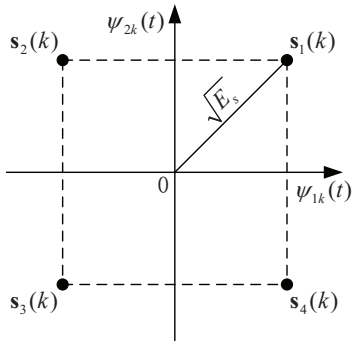

Fig. 1. QPSK signal constellation.

The two components of $\mathbf{n}(k)$ are

$$\begin{cases} n_1(k) = \frac{1}{\sqrt{2T_m}} \int_0^{T_m} n_{ck}(t)dt \\ n_2(k) = \frac{1}{\sqrt{2T_m}} \int_0^{T_m} n_{sk}(t)dt \end{cases} \tag{11}$$

where $n_{ck}(t)$ and $n_{sk}(t)$ are the in-phase and quadrature components of $n(t)$ respectively, i.e., $n(t) = n_{ck}(t)\cos(2\pi f_c(k)t) - n_{sk}(t)\sin(2\pi f_c(k)t)$. From (11), it is easy to show that $n_1(k)$ and $n_2(k)$ are independent and identically distributed Gaussian random variables with zero mean and variance $\frac{N_0}{2}$. When the channel is jamming-free, the outputs of QPSK demodulator follow Gaussian distribution $\mathbf{y}_m(k) \sim \mathcal{N}(\mathbf{s}_m(k),\ \frac{N_0}{2}\mathbf{I})$.

If Strategy I is used, $\mathbf{j}(k) = \mathbf{0}$ when $f_j(k) \neq f_c(k)$. When $f_j(k) = f_c(k)$, the two components of $\mathbf{j}(k)$ are

$$\begin{cases} j_1^{\mathrm{I}}(k) = \sqrt{E_j}\cos\theta \\ j_2^{\mathrm{I}}(k) = \sqrt{E_j}\sin\theta \end{cases} \tag{12}$$

If Strategy II is used, the two components of $\mathbf{j}(k)$ are

$$\begin{cases} j_1^{\mathrm{II}}(k) = \sqrt{\frac{E_j}{N}}\cos\theta \\ j_2^{\mathrm{II}}(k) = \sqrt{\frac{E_j}{N}}\sin\theta \end{cases} \tag{13}$$

Obviously, when the received signal contains additive white Gaussian noise and deterministic interference, the outputs of

QPSK demodulator follow Gaussian distribution $\mathbf{y}_m(k) \sim \mathcal{N}(\mathbf{s}_m(k)+\mathbf{j}(k),\ \frac{N_0}{2}\mathbf{I})$. To find the best anti-jammer under the worst jamming case, we design the minimax anti-jammer which is shown in the next section.

III. Minimax Anti-Jammer Design

Since the symbol error probability is the most important measure to evaluate the performance of the QPSK communication system, the aim of the anti-jammer is to minimize it while the jammer's goal is to maximize it. The best anti-jammer under the worst jamming case can be obtained by solving a minimax optimization problem, in which the objective function is the maximum symbol error probability of the two jamming strategies. Denote symbol error probability by $P_e(\cdot)$. The jammer may change $P_e(\cdot)$ via $\mathbf{j}(k)$, and the anti-jammer may change $P_e(\cdot)$ via decision thresholds. Let ξ_k and η_k denote the decision thresholds along $\psi_{1k}(t)$ and $\psi_{2k}(t)$ respectively. Then, the symbol error probability is a function of ξ_k, η_k, $j_1(k)$, and $j_2(k)$. We omit k for simplicity. Then, symbol error probability is denoted by $P_e(\xi,\eta,j_1,j_2)$.

From (6), we know that the jammer may attack the channel via two strategies, and the jamming signal may use different phases for each strategy. When Strategy I is used, the probability of $f_j(k)=f_c(k)$ is $\frac{1}{N}$, and the probability of $f_j(k)\neq f_c(k)$ is $\frac{N-1}{N}$. The symbol error probability of Strategy I is

$$P_e^{\mathrm{I}} = \frac{1}{N}P_e(\xi,\eta,j_1^{\mathrm{I}},j_2^{\mathrm{I}}) + \frac{N-1}{N}P_e(\xi,\eta,0,0) \tag{14}$$

where j_1^{I} and j_2^{I} are shown in (12).

When Strategy II is used, the symbol error probability is

$$P_e^{\mathrm{II}} = P_e(\xi,\eta,j_1^{\mathrm{II}},j_2^{\mathrm{II}}) \tag{15}$$

where j_1^{II} and j_2^{II} are shown in (13). Note that j_1 and j_2 depend on phase θ for both strategies.

The minimax anti-jammer can be formulated as

$$\min_{\xi,\eta}\max_{i,j_1,j_2} P_e^i \tag{16}$$

To solve this minimax optimization problem, we need to derive the closed-form of $P_e(\xi,\eta,j_1,j_2)$. We know that the received signal contains two binary phase modulation signals along in-phase and quadrature carriers respectively. With perfect orthonormal basis as in (8), there is no crosstalk or interference between the signals on the in-phase and quadrature carriers [10]. Therefore, if Gray encoding is adopted, the symbol error probability of QPSK has the following relationship with bit error probabilities.

$$P_e(\xi,\eta,j_1,j_2) = 1-[1-P_{b\xi}(\xi,j_1)]\,[1-P_{b\eta}(\eta,j_2)] \tag{17}$$

where $P_{b\xi}(\xi,j_1)$ denotes bit error probability on the in-phase carrier $\psi_{1k}(t)$, $P_{b\eta}(\eta,j_2)$ denotes bit error probability on the quadrature carrier $\psi_{2k}(t)$.

Now, we derive the bit error probability $P_{b\xi}(\xi,j_1)$. Since two bits represent one symbol in QPSK, the energy per bit E_b is one half of E_s. From (10), we have $s_{1m}(k)=\sqrt{E_b}$ when $m=1,4$, and $s_{1m}(k)=-\sqrt{E_b}$ when $m=2,3$. Hence, $y_{1m}(k)\sim\mathcal{N}(\sqrt{E_b}+j_1,\ \frac{N_0}{2})$ when $m=1,4$, and $y_{1m}(k)\sim\mathcal{N}(-\sqrt{E_b}+j_1,\ \frac{N_0}{2})$ when $m=2,3$. The PDFs of signals $\mathbf{y}_m(k)$ $(m=1,2,3,4)$ on the in-phase carrier $\psi_{1k}(t)$ are shown in Fig. 2.

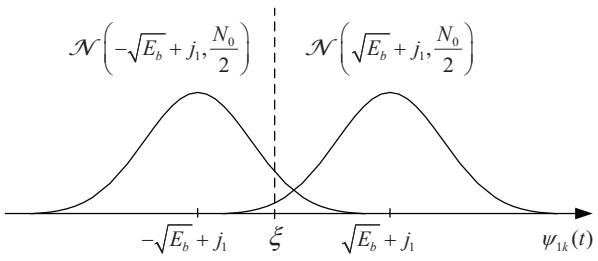

Fig. 2. The PDFs of signals $\mathbf{y}_m(k)$ on the in-phase carrier $\psi_{1k}(t)$.

From Fig. 2, we can derive the bit error probability $P_{b\xi}(\xi,j_1)$ as follows

$$\begin{aligned}
P_{b\xi}(\xi,j_1) &= \frac{1}{2}\int_{-\infty}^{\xi}\frac{1}{\sqrt{\pi N_0}}e^{-\frac{(y_a-\sqrt{E_b}-j_1)^2}{N_0}}dy_a \\
&\quad+\frac{1}{2}\int_{\xi}^{+\infty}\frac{1}{\sqrt{\pi N_0}}e^{-\frac{(y_b+\sqrt{E_b}-j_1)^2}{N_0}}dy_b \\
&= \frac{1}{2}\int_{\frac{\sqrt{E_b}+j_1-\xi}{\sqrt{\frac{N_0}{2}}}}^{+\infty}\frac{1}{\sqrt{2\pi}}e^{-\frac{u_a^2}{2}}du_a \\
&\quad+\frac{1}{2}\int_{\frac{\sqrt{E_b}-j_1+\xi}{\sqrt{\frac{N_0}{2}}}}^{+\infty}\frac{1}{\sqrt{2\pi}}e^{-\frac{u_b^2}{2}}du_b
\end{aligned} \tag{18}$$

where $y_a\in\{y_{11},y_{14}\}$ and $y_b\in\{y_{12},y_{13}\}$. Using the definition of Q-function $Q(x)=\frac{1}{\sqrt{2\pi}}\int_x^{+\infty}e^{-\frac{u^2}{2}}du$, the bit error probability $P_{b\xi}(\xi,j_1)$ can be represented as follows

$$P_{b\xi}(\xi,j_1) = \frac{1}{2}Q\left(\frac{\sqrt{E_b}+j_1-\xi}{\sqrt{\frac{N_0}{2}}}\right)+\frac{1}{2}Q\left(\frac{\sqrt{E_b}-j_1+\xi}{\sqrt{\frac{N_0}{2}}}\right) \tag{19}$$

By using the same method, it is easy to show that the bit error probability $P_{b\eta}(\eta,j_2)$ is as follows

$$P_{b\eta}(\eta,j_2) = \frac{1}{2}Q\left(\frac{\sqrt{E_b}+j_2-\eta}{\sqrt{\frac{N_0}{2}}}\right)+\frac{1}{2}Q\left(\frac{\sqrt{E_b}-j_2+\eta}{\sqrt{\frac{N_0}{2}}}\right) \tag{20}$$

Substituting (19) and (20) into (17), we have the closed-form of $P_e(\xi,\eta,j_1,j_2)$. Then, P_e^{I} and P_e^{II} will be obtained by substituting (17) into (14) and (15). By solving the minimax optimization problem in (16), we will have the worst-case optimal anti-jammer.

IV. Numerical Results

In this numerical example, we solve the minimax problem in (16). By solving this problem, we will know what the optimal anti-jammer is when it is under the worst case jamming attack, and which strategy and phase the jammer will use if it knows the anti-jammer's decision thresholds. Since j_1 and j_2 are the

only functions of θ, we maximize P_e^i respect to θ instead of j_1 and j_2, where $\theta = \frac{l\pi}{32}$, $l = 0, 1, 2, \ldots, 31$. The starting guess of the optimal solution is $\xi = \eta = 0$.

Let $\frac{E_s}{E_j} = 0.5$, $\frac{E_s}{N_0} = 20$, and $N = 5$. By solving (16), we have the following results: the optimal solution is $\xi = \eta = 0$ and $\theta \in \{0, \frac{\pi}{2}, \pi, \frac{3\pi}{2}\}$, the optimum objective value is $P_e = 0.1592$. When the anti-jammer has no knowledge about jamming phase θ, no matter which strategy the jammer uses, the optimum decision thresholds for anti-jammer are $\xi = \eta = 0$. If the jammer knows how the anti-jammer designs decision thresholds, the best choice of the jammer under this setting is using Strategy II and $\theta \in \{0, \frac{\pi}{2}, \pi, \frac{3\pi}{2}\}$. To get this optimal solution, the jammer needs to know $\frac{E_s}{E_j}$, $\frac{E_j}{N_0}$, and the anti-jammer's decision rule. Note that (16) has more than one optimal solution. To show the optimum solution for the jammer, we plot the optimum objective values of P_e^i with different jamming phases in Fig. 3. Obviously, the optimal solution of P_e^i are periodic functions of θ with period $\frac{\pi}{2}$. Because the QPSK signal constellation is symmetric, which is shown in Fig. 1, the effect of $\mathbf{j}(k)$ is periodic with period $\frac{\pi}{2}$. More specifically, P_e^{I} is maximized when $\theta \in \{\frac{\pi}{4}, \frac{3\pi}{4}, \frac{5\pi}{4}, \frac{7\pi}{4}\}$ and P_e^{II} is maximized when $\theta \in \{0, \frac{\pi}{2}, \pi, \frac{3\pi}{2}\}$. It is easy to explain for Strategy II. When $\theta \in \{0, \frac{\pi}{2}, \pi, \frac{3\pi}{2}\}$ and decision thresholds are fixed, $\mathbf{j}(k)$ on the in-phase or quadrature carrier is the largest, which can be figure out from Fig. 2. Hence, the symbol error probability is the largest when $\theta \in \{0, \frac{\pi}{2}, \pi, \frac{3\pi}{2}\}$. Fig. 3 also shows that $\max P_e^{\mathrm{I}} < \max P_e^{\mathrm{II}}$ at the optimal solution, which means that jammer can cause more serious interference by applying Strategy II under this setting.

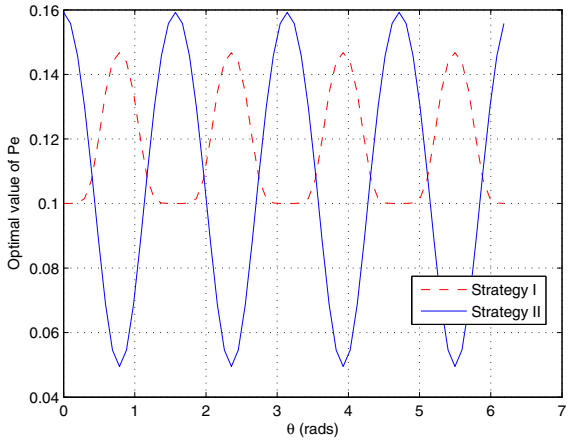

Fig. 3. Optimum objective value of P_e for two strategies with different jamming phases, where $\frac{E_s}{E_j} = 0.5$, $\frac{E_s}{N_0} = 20$, and $N = 5$.

Now, we increase $\frac{E_s}{E_j}$ to 1.25 and show the optimal solution under this setting. By solving (16), we have the following results: the optimal solution is $\xi = \eta = 0$ and $\theta \in \{0, \frac{\pi}{2}, \pi, \frac{3\pi}{2}\}$, the optimum objective value is $P_e = 0.0882$. If the jammer knows how the anti-jammer obtains decision thresholds, the best strategy for the jammer becomes Strategy I under this setting. The optimum objective values of P_e^i with different jamming phases are shown in Fig. 4. Obviously, both P_e^{I} and P_e^{II} are maximized when $\theta \in \{0, \frac{\pi}{2}, \pi, \frac{3\pi}{2}\}$. Comparing Fig. 4 with Fig. 3, the maximum positions of P_e^{I} shift $\frac{\pi}{4}$. More specifically, if the working frequency is attacked, $\theta \in \{\frac{\pi}{4}, \frac{3\pi}{4}, \frac{5\pi}{4}, \frac{7\pi}{4}\}$ will be the optimal solution when the jammer's power is relatively high comparing with the anti-jammer's power; otherwise, $\theta \in \{0, \frac{\pi}{2}, \pi, \frac{3\pi}{2}\}$ will be the optimal solution. We can explain it as follows: when $\frac{E_s}{E_j} = 1.25$, $\sqrt{\frac{E_j}{E_b}} \approx 1.26$ which is not large enough, the jammer needs to fully utilize the limited power by making $\mathbf{j}(k)$ on the in-phase or quadrature carrier is the largest, so $\theta \in \{0, \frac{\pi}{2}, \pi, \frac{3\pi}{2}\}$ is the optimal solution; when $\frac{E_s}{E_j} = 0.5$, $\sqrt{\frac{E_j}{E_b}} = 2$, the projection of $\mathbf{j}(k)$ on the in-phase or quadrature carrier is smallest when $\theta \in \{\frac{\pi}{4}, \frac{3\pi}{4}, \frac{5\pi}{4}, \frac{7\pi}{4}\}$, which is about 1.41 and it is still large, then $\theta \in \{\frac{\pi}{4}, \frac{3\pi}{4}, \frac{5\pi}{4}, \frac{7\pi}{4}\}$ becomes the best solution for the jammer.

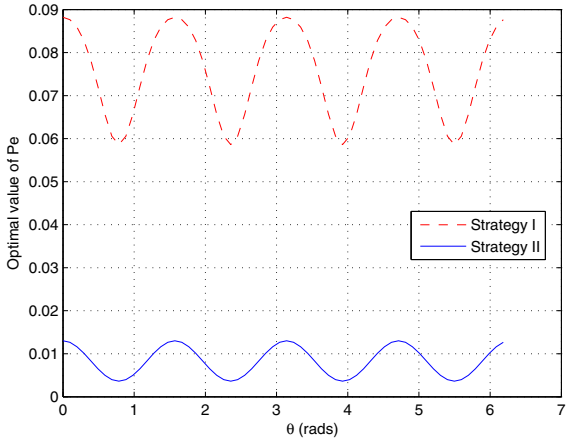

Fig. 4. Optimum objective value of P_e for two strategies with different jamming phases, where $\frac{E_s}{E_j} = 1.25$, $\frac{E_s}{N_0} = 20$, and $N = 5$.

To analyze why the optimal solution is $\xi = \eta = 0$ and $\theta \in \{0, \frac{\pi}{2}, \pi, \frac{3\pi}{2}\}$, we show the maximum P_e between two strategies in ξ-η-θ space in Figs. 5, 6, and 7. First, the function needs to be maximized respect to θ. From Figs. 5 and 6, we know that this function is maximized when θ is close to $\frac{n\pi}{2}, n = 0, 1, 2, 3$. Second, the function needs to be minimized respect to ξ and η. From Fig. 7, we know that this function has minimum value when (ξ, η) is close to $(0, 0)$. This is why the optimum solution of (16) is $\xi = \eta = 0$ and $\theta \in \{0, \frac{\pi}{2}, \pi, \frac{3\pi}{2}\}$.

To compare the optimal value of P_e between two strategies and evaluate the performance under different settings, we change $\frac{E_s}{E_j}$, $\frac{E_s}{N_0}$, or N to get numerical results. By changing $\frac{E_s}{E_j}$, we have Fig. 8. The optimal value of P_e is inversely proportional to $\frac{E_s}{E_j}$ under both strategies. Furthermore, as $\frac{E_s}{E_j}$ increases, Strategy I becomes better choice for the jammer than Strategy II. In other words, it is better for the jammer to choose single-tone jamming when jamming power is low. We also know that anti-jammer can reduce symbol error probability

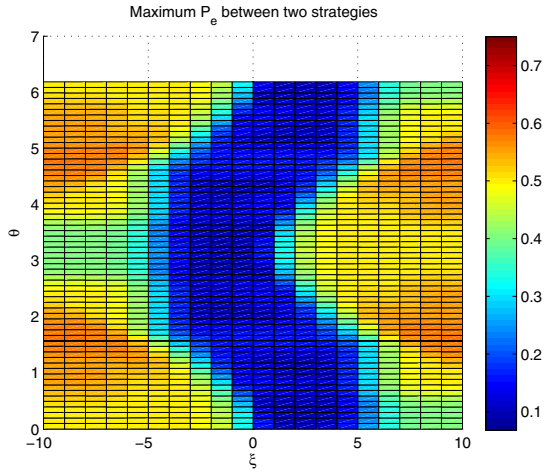

Fig. 5. Maximum P_e between two strategies shown in ξ-θ space when $\eta = 0$, where $\frac{E_s}{E_j} = 0.5$, $\frac{E_s}{N_0} = 20$, and $N = 5$.

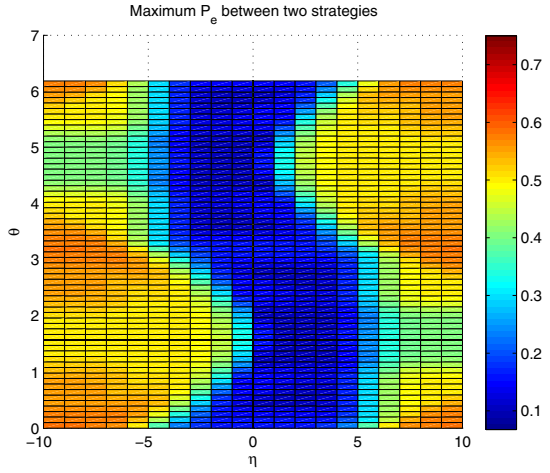

Fig. 6. Maximum P_e between two strategies shown in η-θ space when $\xi = 0$, where $\frac{E_s}{E_j} = 0.5$, $\frac{E_s}{N_0} = 20$, and $N = 5$.

by increasing signal power. By changing $\frac{E_s}{N_0}$, we get Fig. 9. The behavior of Strategy II under different $\frac{E_s}{N_0}$ is similar to that under different $\frac{E_s}{E_j}$. But the performance of Strategy I is nearly constant when SNR is between 8dB and 20dB. From Fig. 9, we also know that Strategy I is a better choice for the jammer when SNR is high and Strategy II is a better choice for the jammer when SNR is low. In this paper, we define signal to interference plus noise ratio (SINR) as $\frac{E_s}{E_j+N_0}$. Figs. 10 and 11 show the optimal value of P_e vs. SINR, which are under the same settings as in Figs. 8 and 9 respectively.

By changing N, we obtain Fig. 12. The optimal value of P_e is inversely proportional to N under both strategies, which indicates that the anti-jammer is able to reduce symbol error probability by increasing the number of frequency hopping channels. From Fig. 12, we also know that Strategy I is preferred by the jammer when N is large and Strategy II is

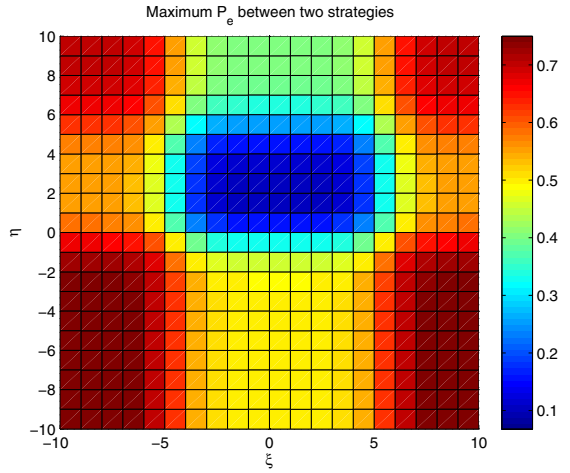

Fig. 7. Maximum P_e between two strategies shown in ξ-η space when $\theta = \frac{\pi}{2}$, where $\frac{E_s}{E_j} = 0.5$, $\frac{E_s}{N_0} = 20$, and $N = 5$.

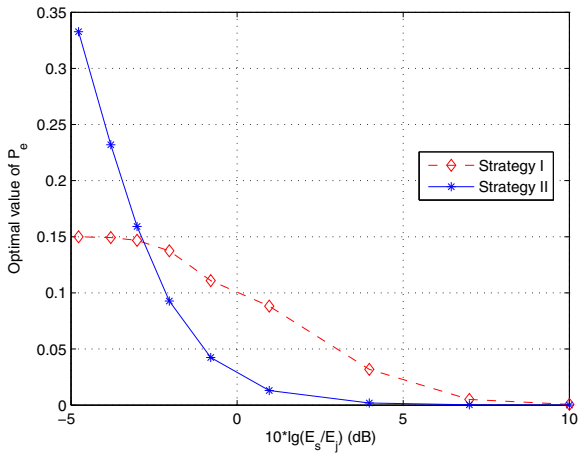

Fig. 8. Optimal value of P_e vs. $\frac{E_s}{E_j}$, where $\frac{E_s}{N_0} = 20$ and $N = 5$.

preferred by the jammer when N is small.

V. Conclusion

In this paper, we designed a minimax anti-jammer for FHSS/QPSK satellite communication system. Two jamming strategies are evaluated: single-tone jamming and full-band multitone jamming. For each strategy, the phase of the jamming signal can be changed. The anti-jammer resists attacks from the jammer by choosing the optimal decision thresholds. The symbol error probability corresponding to each jamming strategy with different jamming phases when different decision thresholds are used is derived. By solving this minimax optimization problem, we know that the best decision thresholds for the anti-jammer when it has no prior knowledge of the phase of the jamming signal are the same as those when received signals are not attacked by the jammer, and the anti-jammer can reduce the symbol error probability by increasing signal power or employing more frequency hopping channels.

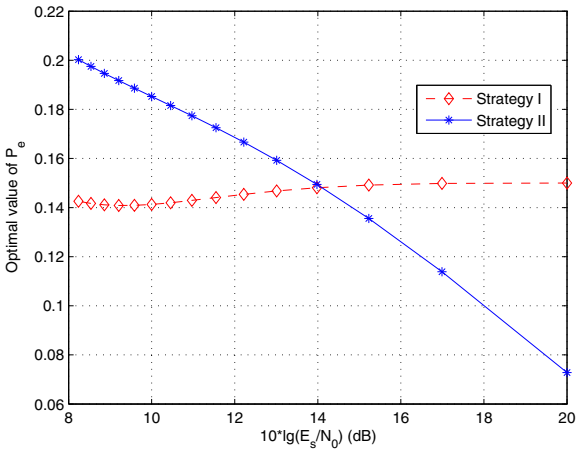

Fig. 9. Optimal value of P_e vs. $\frac{E_s}{N_0}$, where $\frac{E_s}{E_j} = 0.5$ and $N = 5$.

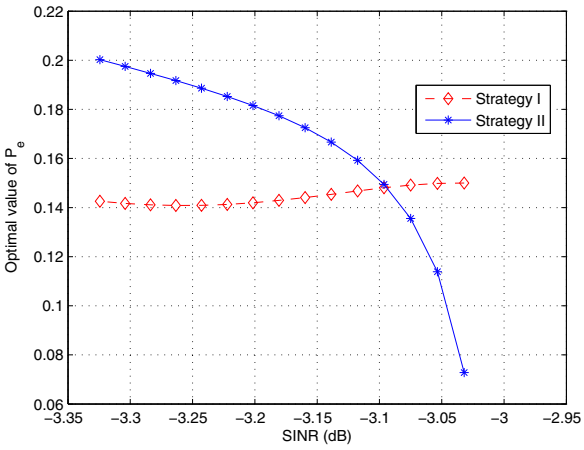

Fig. 11. Optimal value of P_e vs. SINR, where $\frac{E_s}{E_j} = 0.5$ and $N = 5$.

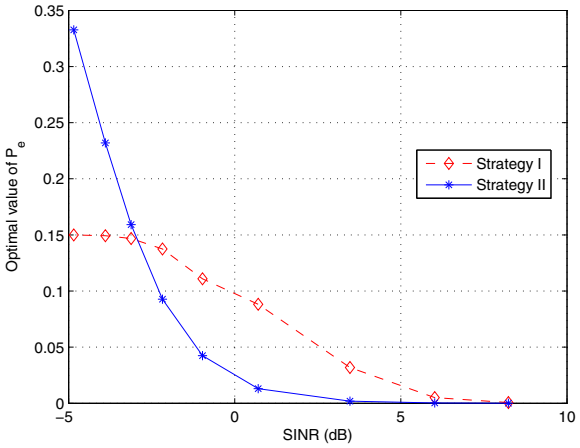

Fig. 10. Optimal value of P_e vs. SINR, where $\frac{E_s}{N_0} = 20$ and $N = 5$.

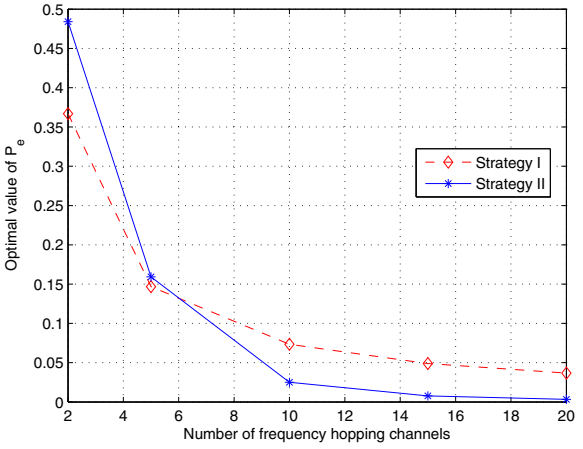

Fig. 12. Optimal value of P_e vs. number of frequency hopping channels, where $\frac{E_s}{E_j} = 0.5$ and $\frac{E_s}{N_0} = 20$.

If the jammer knows the anti-jammer's minimax decision thresholds, the best choice for the jammer is using single-tone jamming when the jamming power is low or N is large, and single-tone jamming will cause nearly constant P_e to the legitimate communication system under different SNRs.

REFERENCES

[1] A. Alagil, M. Alotaibi, and Y. Liu, "Randomized positioning DSSS for anti-jamming wireless communications," in *2016 International Conference on Computing, Networking and Communications (ICNC)*, Feb 2016, pp. 1–6.

[2] S. Fang, Y. Liu, and P. Ning, "Wireless communications under broadband reactive jamming attacks," *IEEE Transactions on Dependable and Secure Computing*, vol. 13, no. 3, pp. 394–408, May 2016.

[3] E. B. Felstead and R. J. Keightley, "Performance of multiple-access frequency-hopped systems in the presence of spurious tones," in *MILCOM 2006 - 2006 IEEE Military Communications conference*, Oct 2006, pp. 1–7.

[4] G. Wang, G. Chen, D. Shen, X. Tian, K. Pham, and E. Blasch, "Spread spectrum design for aeronautical communication system with radio frequency interference," in *2015 IEEE/AIAA 34th Digital Avionics Systems Conference (DASC)*, Sept 2015, pp. 2F1–1–2F1–11.

[5] R. Mathis and R. Pawula, "A spread spectrum system with frequency hopping and sequentially balanced modulation - part II: Operation in jamming and multipath," *IEEE Transactions on Communications*, October 1980.

[6] M. Simon and A. Polydoros, "Coherent detection of frequency-hopped quadrature modulations in the presence of jamming - part I: QPSK and QASK modulations," *IEEE Transactions on Communications*, vol. 29, no. 11, pp. 1644–1660, November 1981.

[7] Q. Chen, Q. Wang, V. K. Bhargava, and L. J. Mason, "Error performance of coded SFH/DPSK in tone interference and AWGN," *IEE Proceedings I - Communications, Speech and Vision*, vol. 140, no. 4, pp. 262–268, Aug 1993.

[8] R. Ghareeb and A. Yongacoglu, "Performance analysis of frequency hopped/coherent MPSK in the presence of multitone jamming," *IEEE Transactions on Communications*, vol. 44, no. 2, pp. 152–155, Feb 1996.

[9] X. Tian, Z. Tian, K. Pham, E. Blasch, and D. Shen, "Jamming/anti-jamming game with a cognitive jammer in space communication," in *SPIE Defense, Security, and Sensing*. International Society for Optics and Photonics, 2012, pp. 83 850Q–83 850Q–10.

[10] J. Proakis and M. Salehi, *Fundamentals of Communication Systems*, 2nd ed. Pearson Education, 2013.